Surface & Coatings Technology 204 (2010) 2813–2816

Contents lists available at ScienceDirect

Surface & Coatings Technology

journal homepage: www.elsevier.com/locate/surfcoat

Protective $Si_xO_yC_z$ coatings on steel prepared by plasma activated chemical vapour deposition

C.A. Lasorsa [a,b,*], P.M. Perillo [a,b], P.J. Morando [c]

[a] Gerencia de Área Investigación y Aplicaciones no Nucleares, Comisión Nacional de Energía Atómica, Avda. Libertador 8250, Buenos Aires 1429, Argentina
[b] Universidad Tecnológica Nacional, Facultad Regional Haedo, Argentina
[c] Gerencia Química, Comisión Nacional de Energía Atómica and Instituto de Tecnología Jorge A. Sabato, UNSAM, Avda. Gral Paz 1499, 1650 San Martín, Buenos Aires, Argentina

ARTICLE INFO

Article history:
Received 16 July 2009
Accepted in revised form 18 February 2010
Available online 3 March 2010

Keywords:
Corrosion
PACVD
MTMOS
Silica-based coating

ABSTRACT

The aim of this paper is to analyze the protective character of $Si_xO_yC_z$ coatings deposited on steel. Coatings were deposited by r.f. plasma assisted chemical vapour deposition using methyltrimethoxy-silane (MTMOS) as precursor in a gaseous mixture of O_2. The process is developed in two stages, first with the substrate at 500 °C and in the second stage with the substrate at room temperature. The first stage is made with the mixture of O_2 and MTMOS, in the second stage a potential of BIAS in the substrate without varying the mixture of gases is added shrouds of the plasma. Surface chemical and morphological characterization of coatings was carried out by Fourier transform infrared spectroscopy (FTIR), X-ray photoelectron spectroscopy (XPS), scanning electron microscopy (SEM) and corrosion test measurements.
The corrosion protective behaviour of the film was determined by potentiodynamics polarization curves with coated probes and without coating, in 5% H_2SO_4 and NaCl 0.1 N solution in nitrogen atmosphere, at room temperature.
The new process was successful in producing coatings with good adhesion and the properties are compatible with good corrosion resistance. The deposition process and the film properties are discussed.

1. Introduction

Amorphous $Si_xO_yC_z$ films provide excellent corrosion protection of steel, which is explained, on the one hand, by a tiny porosity rate, and on the other hand, by intrinsic insulating properties of the coating. This barrier effect avoids any galvanic coupling deleterious to the uncoated metallic surface, and is correlated with the $Si_xO_yC_z$-like character of the film.

Low-temperature deposition of SiO_2 and $Si_xO_yC_z$ thin films by plasma enhanced chemical vapour deposition (PECVD) for applications which require a low substrate temperature (≤100 °C), such as in the manufacture of water-repellent silicon films [1], of microelectronic, optoelectronic and energy conversion devices [2], and coatings for abrasion protection of plastic ophthalmic lenses [3,4], among others.

In these processes, a gaseous mixture of a volatile organosilicon compound with suitable reactive additives is used in addition to silicon, the monomers contain C, H, and O or N atoms forming a complex chemical structure. In contact with the plasma, the monomer is fragmented and forms highly reactive species (activated molecules and atoms, ions, radicals), which mix with the added gases and react both on the gaseous phase as well as on substrate surface to form the film.

The chemistry of formation of SiO_2 and $Si_xO_yC_z$, under low-temperature conditions [5–8] differs significantly from the conditions that prevail for the same process at high temperature. For high temperature, Si–O–Si bonding is dominantly, leading to the formation of hard SiO_2 film. On the other hand, at low temperature, Si–OH (silanol) formation in the plasma becomes important under certain conditions [9,10], and large amounts of this compound may be incorporated into the film, producing a soft gel-like coating [4,11,12].

In this multilayer coating, both processes are combined, one coat deposited at high temperature (≥500 °C), that it acts as an interphase of anchorage between the metallic substrate and the second layer, and a second layer at low temperature (≤100 °C), that constitutes the film of anticorrosive protection [13].

2. Experimental details

The CVD plasma reactor is shown schematically in Fig. 1. It was constructed using a cylindrical pyrex tube (15 cm I.D., 100 cm length) as the vacuum chamber, with the O_2 inlet at one end and the pumping port at the other end. The silicon monomer and the O_2 were introduced through a small nozzle located near the evacuation end of the tube, some 10 cm ahead of the substrate. This gas and monomer inlet configuration allowed for a better control of the plasma activation

* Corresponding author. Gerencia de Área Investigación y Aplicaciones no Nucleares, Comisión Nacional de Energía Atómica, Avda. Libertador 8250, Buenos Aires 1429, Argentina.
E-mail address: lasorsa@cnea.gov.ar (C.A. Lasorsa).

0257-8972/$ – see front matter © 2010 Elsevier B.V. All rights reserved.
doi:10.1016/j.surfcoat.2010.02.054

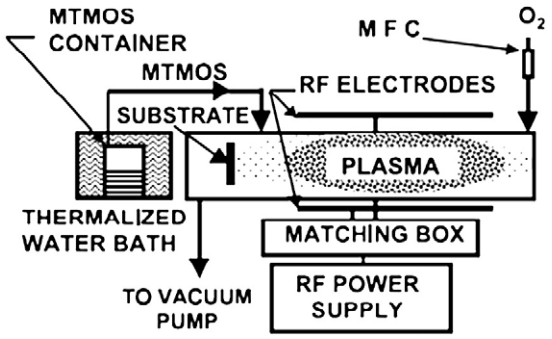

Fig. 1. Schematic illustration of the PECVD reactor.

reactions near the substrate, driven mainly by the electrons and oxygen species coming from the plasma at the midsection of the vacuum chamber. The plasma was formed using a 1-kW RF (13.56 MHz) power supply, coupled capacitively to the gas by external electrodes located at the tube midsection. The plasma extended downstream to the section where the monomer and the O_2 were introduced. The steel (AISI M2) substrate ($10\times15\times5$ mm) was supported facing the plasma outside of the main discharge region, and received the flux of activated species coming from the low electron density and temperature region in front of it. The substrate temperature could be measured using a thermocouple placed on its supporting plate, but no direct temperature control was available. O_2 was added to the monomer vapour in order to control the film properties. O_2 is necessary to control the film Si/O ratio and achieve $Si_xO_yC_z$-like hardness. By proper control of the flow rate of the added gases, it is thus possible to obtain a graded film composition in the direction perpendicular to the substrate, ranging from an elastic and moderately soft material at the base layer to a hard and determined using a capacitive gauge. The monomer source was contained in a glass bottle placed in an automatically thermalized water bath (Yamato Thermo-Mate BF200) at a fixed temperature of 50 °C in order to keep its vapour pressure constant. Under these conditions, coatings were produced and characterized. Several deposition conditions (monomer pressure, flow rate of additional gases, total gaseous $Si_xO_yC_z$-like material at the outer layer, the oxygen flows were measured using automatic mass flow controller (MFC), while the monomer flow could be deduced from the pressure rise in the chamber with respect to the initial added gases pressure, which was mixture pressure, RF power) were tried in order to optimize the film properties.

2.1. Coating deposition

The steel specimens are polished with 600 grit emery papers before the ultrasonic cleaning.

Films were deposited in two layers on a grit-polished steel. The substrate material is a high speed steel (AISI M2) composed of 0.95 wt.% C, 0.24 wt.% Si, 4.5 wt.% Cr, 0.3 wt.% Mn, 4.5 wt.% Mo, 4.5 wt.% W and 1.6 wt.% V and the balance being Fe.

$Si_xO_yC_z$ coatings were prepared by r.f. PACVD using methyltrimethoxy-silane as precursor, and the contribution of O_2 as reactive gas. The temperature is measured by a thermocouple close to the sample. In the first process it exceeds 500 °C without BIAS potential. In the second process, the work pressure and the flows of precursor and O_2 are conserved, taking the temperature of the substrate to 100 °C, and equipping it with potential of BIAS (+100 V). The separation between the injector of the precursor and the substrate is 5 cm.

Table 1 shows the parameters of the process.

2.2. Characterization

The coating chemical elements and their bonding condition were characterized using X-ray photoelectron spectroscopy (XPS) [14] (Vacuum Generator Mod. ESCA 3 MARK II) The X-ray in XPS was generated at 10 kV and 20 mA, using Mg Kα radiation ($h\nu=1253.6$ eV). The air pressure in the vacuum chamber was 7×10^{-9} Torr. The depth profile analyses of the near surface regions were carried out by sputtering with Ar^+ ions using a current intensity of 6 μA and an acceleration voltage of 5 kV (ion current, 8 μA) at an argon pressure of 8×10^{-5} mTorr.

The XPS was corrected for charge shifting by taking C 1s at 285.0 eV. All the experiments were conducted at room temperature.

Spectra of Si 2p, O 1s and C 1s were recorded to measure concentration profiles. The C 1s peak with a binding energy (BE) of 284.6 eV was used as reference for the correction of surface charging.

FTIR spectra (for characterisation of film functional groups) of covers obtained were recorded in a Nicolet MAGNA 560 instrument equipped with a liquid N_2 cooled MCT-A detector.

The coating microstructure was characterized by SEM (scanning electronic microscopy) using a FEI model QUANTA 200.

Thickness was measured using a mechanical profilometer (Mitutoyo Mod. Surftest SV-400) and microhardness (Akashi Mod. MVK-H2). In addition, plasma emission optical spectroscopy (OES) (SPEX Mod. 1870 spectrometer) was used in the spectral range 300–500 nm in order to identify the species in the plasma at a distance of 3 cm in front of the substrate surface, as well as to evaluate changes in the emission spectra as the oxygen flow rate was increased.

2.3. Electrochemical measures

Electrochemical measures were obtained using a Gamry PC4/750 potentiostat/galvanostat. Corrosion resistance was determined by potentiodynamics polarization curves with coated probes and without coating, in 5% H_2SO_4 and NaCl 0.1 N solution in nitrogen atmosphere, at room temperature, in conventional corrosion cells. The electrode potential was measured through a Luggin capillary. A saturated calomel electrode (SCE) or sulfate electrode (SE) and a platinum wire (surrounding the specimen) were employed as the reference electrode and the counter electrode, respectively. Before all electrochemical measurements, specimens were held immersed in the solution to reach a stationary corrosion potential for 60 min before testing.

To avoid crevice corrosion a protective acetate lacquer was used to mask the samples, allowing 0.7 cm^2 of their surface to be in contact with the solution. The polarization curves of all the specimens were generated after conducting the scan from −200 mV below corrosion potential at a scan rate of 0.1666 mV/s. The solutions were prepared from analytical grade materials and distilled water.

3. Results and discussion

3.1. Characterization

The rate of deposition obtained, using parameters of Table 1, was 2 μm/h, achieving thickness of 8 μm. XPS is an important tool in the studies of the cover. Many works use this technique for the characterization [14–18] and the optimization of the process of the preparation [14]. In our case its use allowed to observe the presence of

Table 1
Deposition parameters.

	First coating	Second coating
Pressure [mTorr]	120	120
Power [W]	900	600
Temperature [°C]	500	Room temperature
O_2 flow rate [sccm]	200	200
MTMOS flow rate [sccm]	120	120
Time [min]	60	120
BIAS [V]	–	+100

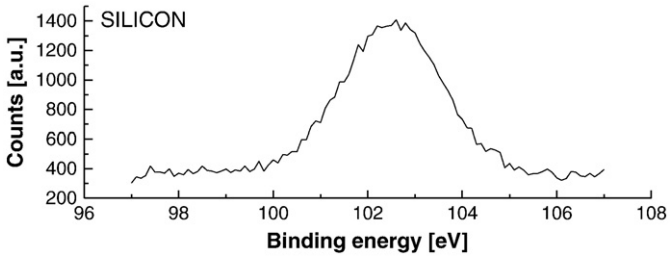

Fig. 2. XPS narrow spectrum corresponding to Si 2p.

Si, O and C. The spectra of individual peaks (narrow) of these elements were analyzed, measured with high energy resolution (Figs. 2–4).

The peak at 102, 6 eV observed in Fig. 2 agrees with the expectable one for the Si–O bond, and differs substantially from the pure Si (99.2 eV) and of other oxides such as Si_2O (100.9 eV) and Si_2O_3 (103.1 eV) [19].

On the other hand, the characteristic peak at 100.3 eV of Si–C union is not observed.

The formation of SiO_2 is also supported by the O 1s spectrum, illustrated in Fig. 3, which presents a well defined peak with a binding energy of 532.4 ± 0.1 eV typical of the combination of oxygen with silicon to form silicon dioxide.

Fig. 4 shows the deconvoluted spectrum of C 1s. Two peaks were obtained one of them with a binding energy of 285.5 ± 3 eV, attributable to the existence of C–O bonds and the other one, with an energy of 284.1 ± 3 eV, attributable to the C–C bond [14].

Note that not any peak in the zone corresponding to the C–Si union (283.5 eV) is observed. The absence of this peak and the appearance in the ir spectra of carbon species must be attributed to that these were embedded in the matrix. A similar fact has been reported by Ding Shi Jin et al. for covers obtained using fluorinated precursors [16].

Observation of FTIR spectroscopy in single coatings obtained by each one of the processes (at high and low temperature respectively) shows a great difference between the functional groups of the first and second layers. Fig. 5 shows the FTIR spectra for both layers. The band assignation was realised by comparison with bibliography data [20–22]. Both layers show clear differences of composition. The first present in 1090 cm^{-1} is an important peak corresponding to Si–O–Si stretching which is reduced to a shoulder in the second layer. Corresponding in this last, the band due to the SiOH stretching (1000–950 cm^{-1}), that appears very small in the first layer, is remarkably increased. On the other hand both zones of the spectra show that the second layer has an important water content which is observed clearly between 600–900 and 2800–3900 cm^{-1} in spite of which it is possible to see the peak due to the SiOH stretching at 3650 cm^{-1}.

Particular attention deserves two observed peaks and a shoulder between 2800 and 3000 cm^{-1}. The same can be attributed to the presence of CH_3O groups, originating of the MTMOS, adsorbed on the first layer. A similar fact was reported by Deshmukh and Aydil [23], which working with tetraethoxysilane (TEOS) at low temperatures found reversible adsorption of CH_3CH_2O groups.

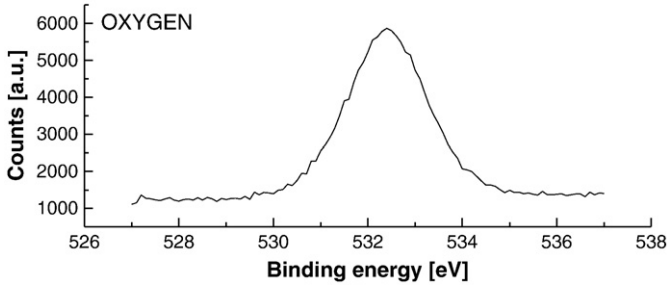

Fig. 3. XPS narrow spectrum of O 1s.

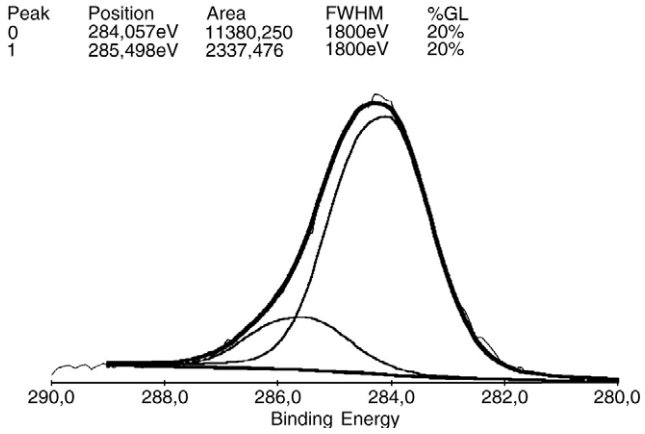

Fig. 4. Narrow spectrum of C 1s (thick line) and peak deconvolution constituents (binding energy: eV; amplitude: A.U.).

The composition of the second layer (important amount of water, adsorbed groups CH_3O, large amount of SiOH group) could suggest that this one was more fragile than the first. In this way, Nguyen et al. [24], found that the speed of etching increases if the deposition takes place to smaller temperatures. Nevertheless in our case the second layer is not only stable in aqueous solutions of high acidity, also it causes important improvements in the corrosion resistance (see below).

Fig. 6 is a SEM cross section view of the coating. The microstructure shows one compact columnar growth which gives it corrosion barrier characteristics.

3.2. Electrochemical tests

References above corrosion protection by covers obtained starting from similar precursors, even if the preparation conditions are different, is scanty. The works of Schreiber et al. and Moretti et al. can be mentioned. The first of these uses the qualitative method of immersion of the surfaces covered in simulated sea water, while the another one uses Electrochemical Impedance Spectroscopy and Secondary Ion Mass Spectrometry. In our work corrosion protection is evaluated by study of the polarization curves and of the corrosion rate of pure and coated steel samples immersed in acidic and saline solutions.

Fig. 7 shows the corrosion rate from both samples and confirms the better corrosion resistance of the coated compared to the pure steel. Current density, during anode scanning, is always lower for the uncoated specimen, which indicates a good protection effect.

Fig. 7 shows potentiodynamic scans of the coated and uncoated steel. In the case of sulfuric acid no significant potential shift was observed between coated and bare substrate (-0.9 V), so that the current density of the bare substrate at the mixed potential ia(Em)

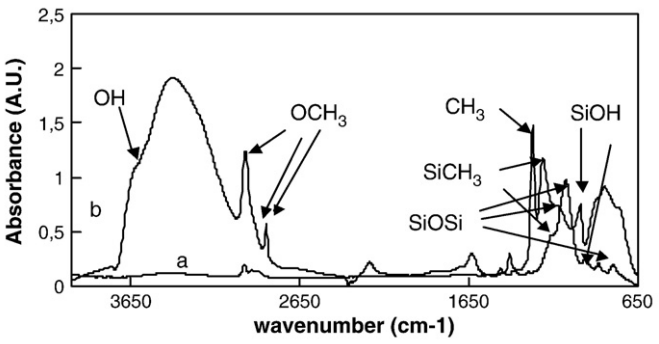

Fig. 5. FTIR spectra in the range 4000–650 cm^{-1} for the first (a) and the second (b) layers.

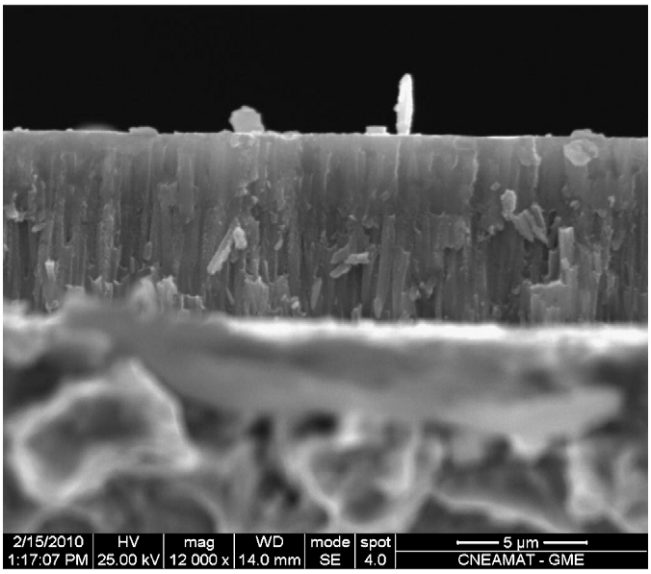

Fig. 6. SEM cross section view of the coating.

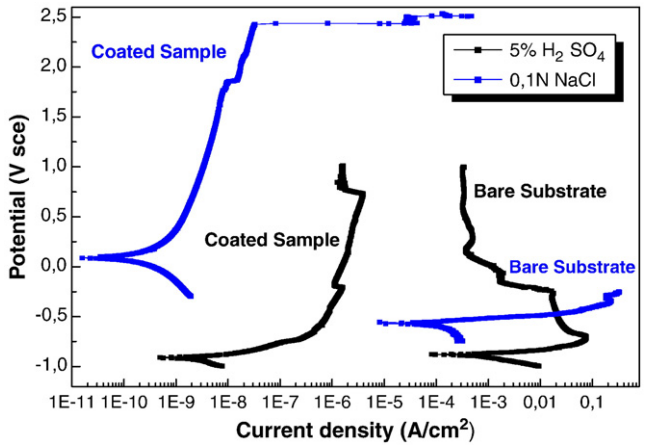

Fig. 7. Polarization curve of bare M2 substrate and coated M2 sample in 5% sulfuric acid solution and in 0.1 N NaCl solution.

corresponds to its simple corrosion current density. The drop of several decades of the current density of coated steel with respect to the substrate showed the beneficial role of the silica-based coating on the degradation rate. The coated substrate was more efficient in preventing the dissolution of the passive layer formed.

On the other hand, in the case of 0.1 N NaCl a more positive corrosion potential value (i.e. less electronegative) and a curve located several decades at low-current density imply better anti-corrosion performance. The corrosion potential of the uncoated steel was found to be −0.55 V significantly less noble than the coated substrate, which was found to have a relative large corrosion potential at 0.10 V.

It is well known that Cl^- ions are aggressive enough to attack steel and initiate pitting. The pitting potential of the bare steel starts very close to the corrosion potential. A breakdown of the passivity, which corresponds to pitting corrosion E_{pit} occurred at high potentials in the coated sample. Its pitting potential is near 2.5 V with a faster increase of the current density.

4. Conclusions

In this study, $Si_xO_yC_z$ film was deposited by r.f. PACVD on steel substrates, with methyltrimethoxy-silane and O_2 gas flow rate in the mixture in two processes, obtaining a bilayer coating. The first process at high temperature (500 °C) without BIAS potential and the second one at low temperature (100 °C) with BIAS potential (+100 V). The coating produced at high temperature acts like anchorage between the metal substrate and the first layer, and the second layer (at low temperature) provides corrosion protection. The electrochemical data obtained in this work indicate that coatings exhibit higher corrosion resistance in sulfuric acid and chlorides that bare substrates. The potential use of BIAS optimizes the process of improving these properties, either in media such as acids in chlorides. From a mechanical point of view, this coating presents good adhesion (tape test) [27], and has a hardness of approximately 1.20 GPa. The results obtained in this work are in qualitative agreement with those obtained by Schreiber [25] and Moretti [26] using a technique more quantitative than the first and less expensive than the another one.

Acknowledgment

The authors gratefully acknowledge Dr Adolfo Rodrigo for technical support.

References

[1] Y. Wu, H. Sugimura, Y. Ionue, O. Takai, Thin Solid Films 435 (2003) 161.
[2] L. Zajıckova, V. Bursıkova, Z. Kucerova, J. Franclova, P. Stahel, V. Perina, A. Mackova, J. Phys. Chem. Solids 68 (2007) 1255.
[3] A. Pfuch, A. Heft, R. Weidl, K. Lang, Surf. Coat. Technol. 201 (2006) 189.
[4] R.-F. Bunshah, et al., (Eds.), Deposition Technologies for Films and Coatings, Noyes Publications, Cap. 2, New Jersey, 1982.
[5] S.K. Rau, C.K. Maiti, S.K. Lahiri, N.B. Chakrabarti, J. Vac. Sci. Technol. B 10 (3) (1992) 1139.
[6] Ch. Bayer, E. Bapin, Ph.R. von Rohr, Surf. Coat. Technol. 116–119 (1999) 874.
[7] A. Pecheur, J. Autran, J. Lazarri, P. Pinard, J. Non-Cryst. Solids 245 (1999) 20.
[8] D. Hegemann, U. Vohrer, C. Oehr, R. Riedel, Surf. Coat. Technol. 116–119 (1999) 1033.
[9] C. Lasorsa, P.J. Morando, A. Rodrigo, Surf. Coat. Technol. 194 (2005) 42.
[10] N. Selamoglu, J. Mucha, D. Ibbotson, D. Flamm, J. Vac. Sci. Technol. B7 (1989) 1345.
[11] S. Menichella, C. Misiano, E. Simonetti, C. DeCarlo, M. Carrabino, 37th Annual Technical Conference Proceedings, Society of Vacuum Coaters, 1994, p. 37.
[12] R. D'Agostino (Ed.), Plasma Deposition, Treatment and Etching of Polymers, Academic Press, New York, 1990.
[13] D. Pech, P. Steyer, A.S. Loir, J.C. Sánchez-López, J.P. Millet, Surf. Coat. Technol. 201 (2006) 347.
[14] P.W. Wang, S. Bater, L.P. Zhang, M. Ascherl, J.H. Craig Jr., Appl. Surf. Sci. 90 (1995) 413.
[15] E.B. Halac, H. Huck, C. Oviedo, M.E. Reinoso, M.A.R. Benyacar, Surf. Coat. Technol. 122 (1999) 51.
[16] S.-J. Ding, P.-F. Wang, W. Zhang, J.-T. Wang, W.W. Lee, Chin. Phys. 10 (2001) 324.
[17] V.V. Kaichev, M. Morkel, H. Unterhalt, I.P. Prosvirin, V.I. Bukthiyarov, G. Rupprechter, H.-J. Freund, Surf. Sci. 566–568 (2004) 1024.
[18] A. Walkiewicz-Pietrzykowska, J.P. Espinós, AgustinR. González-Elipe, J. Vac. Sci. Technol. A 24 (4) (2006) 988.
[19] J. Chastain, R. King (Eds.), Handbook of X-ray Photoelectron Spectroscopy, Physical Electronics, Inc., 1995.
[20] Y. Inoue, O. Takai, Plasma Sources Sci. Technol. 5 (1996) 339.
[21] C. Shashank, Deshmukh, E. Aydil, J. Vac. Sci. Technol. B13 (1995) 2354.
[22] A. Takamatsu, M. Shibata, M. Ishida, H. Sakai, T. Yoshimi, J. Electrochem. Soc. 133 (1985) 443.
[23] C.S. Deshmukh, E.S. Aydil, J. Vac. Sci. Technol. A 13 (1995) 2355.
[24] S. Nguyen, D. Dobuzinsky, D. Harmon, R. Gleason, S. Fridman, J. Electrochem. Soc. 137 (1990) 2209.
[25] H.P. Schreiber, M.R. Wertheimer, A.M. Wrobel, Thin Solids Films 72 (1980) 487.
[26] G. Moretti, F. Guidi, R. Canton, G. Capobianco, A. Glisenti, M. Battagliarin, (2002), "An industrial PECVD application: modified SiO2 films deposited on OT59 brass for wear and corrosion protection", *Proceedings of the 15th International Corrosion Congress*, Granada, 22–27 September, Paper no 582, pp. 208.
[27] D.S. Campbell, in: L.I. Maissel, R. Glang (Eds.), Hambook of Thin Film Technology, McGraw-Hill, New York, 1970, Chap. 12.3.